International Journal of Nanomedicine

Dovepress
open access to scientific and medical research

Open Access Full Text Article

ORIGINAL RESEARCH

Anti-Angiogenic Activity Of Bevacizumab-Bearing Dexamethasone-Loaded PLGA Nanoparticles For Potential Intravitreal Applications

This article was published in the following Dove Press journal:
International Journal of Nanomedicine

Jiaxin Liu
Xueyan Zhang
Ge Li
Fei Xu
Shuang Li
Lesheng Teng
Youxin Li
Fengying Sun

School of Life Sciences, Jilin University, Changchun, Jilin, People's Republic of China

Purpose: Age-related macular degeneration is a multifactorial disease involving inflammation and choroidal neovascularization. Vascular endothelial growth factor (VEGF) has been regarded as a potential therapeutic target to treat choroidal neovascularization. Dexamethasone can interfere with the expression or action of VEGF while bevacizumab targets and combines with VEGF. We propose electrostatically-conjugated bevacizumab-bearing dexamethasone-loaded poly (D,L-lactide-co-glycolide)/polyethylenimine nanoparticles (eBev-DPPNs) for angiogenic combination treatment of ocular diseases.

Methods: We prepared a novel nanoparticle composed of poly (D, L-lactide-co-glycolide) and polyethylenimine and loaded the nanoparticles with dexamethasone. Bevacizumab was adsorbed onto the surfaces of the nanoparticles by electrostatic interactions. The eBev-DPPNs were evaluated according to their size, polydispersity index, zeta potential, morphology, drug loading, release behavior, and stability. The structural stability of bevacizumab on the surface of the nanoparticles was also analyzed. Subsequently, angiogenesis was investigated in the presence of the eBev-DPPNs using cell apoptosis, wound healing, Transwell invasion, and tube formation assays on the human umbilical vein endothelial cells (HUVECs) in vitro and chick embryo chorioallantoic membrane assay in vivo. The eBev-DPPNs intravitreal injection was applied in the laser-induced rabbit choroidal neovascularization (CNV) model to confirm the role for potential intravitreal applications.

Results: The eBev-DPPNs was about 200 nm in diameter, with a narrow diameter distribution, and the surface charge was neutral (0.85 ± 0.37mV), which made the eBev-DPPNs stable under physiological conditions. The apoptosis, migration, invasion, and tube formation assays showed that the eBev-DPPNs had a good anti-angiogenic effect on HUVECs. The eBev-DPPNs also provided a strong inhibitory effect on VEGF secretion from HUVECs. Moreover, in vivo chick embryo chorioallantoic membrane assay showed eBev-DPPNs greatly reduced the amount of blood vessels. The leakage area of CNV decreased in the eBev-DPPNs group on rabbit CNV model.

Conclusion: The eBev-DPPNs are a promising novel anti-angiogenesis therapeutic for potential intravitreal applications such as age-related macular degeneration.

Keywords: nanoparticles, dexamethasone, bevacizumab, anti-angiogenesis, VEGF

Correspondence: Youxin Li; Fengying Sun
School of Life Sciences, Jilin University, 2699 Qianjin Street, Changchun, Jilin 130012, People's Republic of China
Tel/Fax +86 431 8515 5320
Email liyouxin@jlu.edu.cn; sunfengying@jlu.edu.cn

Introduction

Choroidal neovascularization (CNV) is the main cause of vision impairment in age-related macular degeneration (AMD), and AMD has become one of the main causes of blindness worldwide.[1,2] Several factors may trigger CNV, such as vascular endothelial growth factor (VEGF), angiopoietin, basic fibroblast growth factor, and

adhesion molecule (AM). An imbalance between VEGF and anti-angiogenic factors is especially important in triggering CNV.[3] In a normal physiological state, VEGF expression in eye tissues is relatively low, but VEGF expression is significantly increased during ischemia, hypoxia, and inflammation, inducing the formation of pathological blood vessels. Based on this pathophysiology, VEGF has been considered a potential therapeutic target in the treatment of CNV. For example, pegaptanib (Macugen®) is a VEGF aptamer, and ranibizumab (Lucentis®), bevacizumab (Avastin®) and VEGF-trap (Eylea®) are anti-VEGF antibody fragments.[4–8]

In recent years, substantial evidence has highlighted the critical role of immune-inflammatory processes in CNV pathogenesis.[9] Dexamethasone, a corticosteroid, is widely used to treat ophthalmic diseases including diabetic retinopathy, ocular inflammation and CNV.[10] Corticosteroids can act to reduce inflammation rapidly, strongly and non-specifically and interfere with the expression or action of VEGF and other proinflammatory cytokines, induce apoptosis of vascular endothelial cells, and inhibit vascular endothelial proliferation, sequentially.[10,11]

Recently, nanomedical approaches for the diagnosis and theatment of many diseases, including inflammatory and eye diseases, have shown promise.[12–14] Scientists showed great interest in delivering drug to the posterior chamber of the eye by sustained release systems.[15–18] Compared with microspheres and gels, nanoparticles are small and have functionalizable surfaces. The advantage of nanoparticles over implants is that the particles can be delivered through a traditional fine needle to avoid invasive surgery. The advantage of nanoparticles over microspheres is that they can avoid the risk of migrating into the anterior chamber, and mitigate the risk of corneal or initial intraocular pressure (IOP) issues. Poly (lactic-co-glycolic acid) (PLGA) is composed of lactic acid and glycolic acid,[19] and it is used in drug delivery systems due to its biodegradability and biocompatibility. Polyethylenimine (PEI) has been widely used in drug delivery systems due to it proton sponge effect.[20,21] It has been reported that PEI has a high positive charge, making it electrostatically interact with negatively charged molecules.[22]

As previously demonstrated, combination treatment of CNV with steroids and anti-VEGF agents shows potential.[23] In this study, dexamethasone-loaded PLGA/PEI nanoparticles (DPPNs) were prepared and then bevacizumab was subsequently electrostatically adsorbed onto the DPPNs. In addition, chemically-conjugated bevacizumab-bearing dexamethasone-loaded PLGA nanoparticles (cBev-DPNs) were fabricated for comparison. The anti-angiogenic activity of the electrostatically-conjugated bevacizumab-bearing DPPNs (eBev-DPPNs) was investigated using cell apoptosis, migration, invasion, and tube formation assays on the human umbilical vein endothelial cells (HUVECs) in vitro and chick embryo chorioallantoic membrane (CAM) assays in vivo compared with that of dexamethasone, bevacizumab and cBev-DPNs. The eBev-DPPNs intravitreal injection was applied in the laser-induced rabbit CNV model to confirm the role for potential intravitreal applications.

Materials And Methods

Materials

Dexamethasone was purchased from Shanghai Yuanye Bio-Technology Co., Ltd. (Shanghai, China). Bevacizumab (molecular weight (M_W) 149 kDa) was donated by Luye Pharmaceutical Co., Ltd. (Shandong, China). PLGA 7525 2A (lactide/glycolide ratio, 75/25; inherent viscosity 0.22 dL/g) was purchased from Lakeshore Biomaterials (Birmingham, AL, USA). Bicinchoninic acid (BCA) protein assay kits were purchased from Thermo Scientific (Waltham, MA, USA). PEI (M_W 25 kDa, branched), 1-ethyl-3-(3-dimethylaminopropyl) carbodiimide hydrochloride (EDC), N-hydroxysuccinimide sodium salt (NHS) and polyvinyl alcohol (PVA) (M_W, 13–23 kDa) were purchased from Sigma-Aldrich (St Louis, MO, USA). Acetonitrile was purchased from Thermo Fisher Scientific (Waltham, MA, USA). Human VEGF enzyme-linked immunosorbent assay (ELISA) kits were obtained from Elabscience Biotechnology Co., Ltd. (Wuhan, China). All other chemical reagents and solvents used were of analytic reagent grade.

HUVECs were obtained from Procell Biological Technology (Wuhan, China), and were grown in Medium 199 (M199) (Hyclone, Logan, Utach) with 10% foetal bovine serum (Procell, Wuhan, China), 100 U/mL penicillin, and 100 mg/mL streptomycin (Gibco, Grand Island, USA) at 37 °C in a humidified atmosphere of 5% CO_2.

Male New Zealand White rabbits (body weight ~3.0 kg, n = 3) and male Chinchillaf rabbits (body weight ~3.0 kg, n = 15) used in this experiment were approved by the Experimental Animal Ethics Committee of the School of Life Sciences, Jilin University. All rabbits were cared for and treated in accordance with the Association for Research in Vision and Ophthalmology (ARVO) resolution concerning the use of animals in ophthalmological research. Prior to treatment, all animals were free of ocular diseases.

Preparation Of The Nanoparticles

Electrostatic Conjugation Strategy

DPPNs were prepared using an oil in water (O/W) emulsion-solvent evaporation method. Briefly, 20 mg of PLGA was dissolved in 800 μL dichloromethane (DCM) and 4 mg of dexamethasone was dissolved in 200 μL acetone as the organic phase. PEI was dissolved in 5 mL of an aqueous PVA solution (0.5%, w/v), the organic phase was added dropwise, and the mixture was then sonicated (JY 92-IIN, Ningbo Scientific Biotechnology Co. Ltd., China) with a constant power output of 300 W for 3 min in an ice bath. The resulting emulsion was gently stirred with a magnetic stirrer (IKA, German) gently at room temperature for 6 h. Hardened nanoparticles were collected by centrifugation (Allegra 64R, Beckman Coulter, USA), then washed 3 times with distilled water to remove drug and PVA residue. An objective powder was obtained by lyophilization (ALPHA 1–2 LD PLUS, Christ, Osterode am Harz, Germany).

The eBev-DPPNs were prepared by mixing bevacizumab and DPPNs in phosphate buffer solution (PBS) (20 mM, pH 8.0) for 2 h at 25 °C. The reaction mixture was centrifuged at 4000 rpm in an ultrafiltration centrifuge tube with MWCO of 300 kDa (Vivaspin 20, Sartorius, German) to remove free salt ions and unbound bevacizumab. The eBev-DPPNs were obtained after lyophilization.

Chemical Conjugation Strategy

To prepare dexamethasone-loaded PLGA nanoparticles (DPNs), an O/W emulsion-solvent evaporation method was used. Briefly, 20 mg of PLGA was dissolved in 800 μL DCM and 4 mg of dexamethasone was dissolved in 200 μL acetone. This entire mixture was added dropwise to 5 mL of 0.5% PVA solution and sonicated with a constant power output of 300 W for 3 min in an ice bath. The resulting emulsion was then stirred with a magnetic stirrer gently at room temperature for 6 h. Hardened nanoparticles were collected by centrifugation and washed 3 times with distilled water to remove drug and PVA residue. The objective powder was obtained by lyophilization.

The carboxylic groups in the PLGA of the nanoparticles was covalently reacted with the amino groups of bevacizumab using a carbodiimide reaction.[24] Firstly, 10 mg of the above nanoparticles was acidified in 10 mL of 1 M HCl solution. Next, 5 mg of NHS and 20 mg of EDC were added to the nanoparticles and stirred for 4 h at 25 °C, then the activated nanoparticles were collected by centrifugation. Activated nanoparticles and bevacizumab were then incubated in pH 7.4 PBS for 18 h at 25 °C, washed three times with centrifugation to remove unbound bevacizumab and buffer salt ions, collected, and lyophilized. Finally, the reaction mixture was centrifuged at 4000 rpm with an ultrafiltration centrifuge tube with MWCO of 300 kDa to remove free salt ions and unbound bevacizumab. The cBev-DPNs were obtained after lyophilization.

Characterization Of The Nanoparticles

The particle size, polydispersity index (PDI) and zeta potential of the nanoparticles were examined at 25 °C using dynamic light scattering (DLS) (Zetasizer Nano ZS90, Malvern, UK). Prior to detection, nanoparticles were diluted to 1 mg/mL with deionized water.

The surface morphology of the nanoparticles was evaluated using a scanning electron microscope (SEM) (JXA-840, JEOL, Japan) with an electron bean energy of 3 kV. Prior to observation, 1 mg/mL of nanoparticles was placed on a silicon wafer and allowed to dry at room temperature.

The drug loading (DL) and encapsulation efficiency (EE) of dexamethasone in the nanoparticles were determined using high-performance liquid chromatography (HPLC) (2707 auto sampler, 1525 binary HPLC pump, 2487 UV detector, Waters, USA) with an absorption peak of 280nm. Briefly, 10 mg of dexamethasone-loaded nanoparticles was dissolved in 1 mL of DCM and 4 mL of mobile phase (acetonitrile/water = 60:40 (v/v)) was added. DL and EE were calculated as follows:

$$DL\,(\%) = \frac{amount\ of\ dexamethasone\ encasulated\ in\ nanoparticles}{amount\ of\ nanoparticles} \times 100\%$$

$$EE\,(\%) = \frac{actual\ drug\ loading}{theoretical\ drug\ loading} \times 100\%$$

The amount of bevacizumab attached to the surfaces of the DPNs or DPPNs was examined indirectly. Briefly, the solution removed after centrifugation in an ultrafiltration centrifuge tube was collected and analyzed for bevacizumab concentration using BCA assays. The detection wavelength was set to 562 nm (Multiskan Spectrum, Thermo, USA). The binding efficiency (BE) was calculated as follows:

$$BE\ (\%) = \frac{\begin{matrix}initial\ amount\ of \\ bevacizumab\end{matrix} \quad \begin{matrix}-\ amount\ of \\ free\ bevacizumab\end{matrix}}{amount\ of\ nanoparticles} \times 100\%$$

Stability Of The Nanoparticles

The rabbit was executed by injecting air into the ear vein, then the eyeball was removed and the vitreous humor was extracted. Lyophilized eBev-DPPNs or cBev-DPNs were suspended in PBS (20 mM, pH 7.4) or vitreous humor of rabbit eyes, and subsequently incubated at 37 °C. After incubation, free bevacizumab was separated from the nanoparticles and detected with BCA assays. Nanoparticles size, PDI and the amount of dissociated bevacizumab were measured at predetermined time points.

Structural Stability Of The Bevacizumab On The Surface Of The Nanoparticles

Lyophilized eBev-DPPNs or cBev-DPNs were resuspended in PBS (20 mM, pH 7.4) and incubated at 37 °C, then bevacizumab that had dissociated from the surface of the nanoparticles was recycled and filtered with a 0.22-μm aperture for further testing.

The primary, secondary, and tertiary structural stability of bevacizumab was analyzed using size exclusion chromatography (SEC-HPLC), circular dichroism (CD) (J-810, Jasco, USA), and fluorescence spectroscopy (RF-5301, Shimadzu, Japan) as previously described.[25]

In Vitro Drug Release Study

In vitro assays were conducted to study the release of dexamethasone and bevacizumab from the eBev-DPPNs and the cBev-DPNs. Briefly, 10 mg of nanoparticles suspended in 1 mL of PBS (20 mM, pH 7.4) containing 0.5% Tween-80 were sealed in a dialysis bag with MWCO of 8 kDa and incubated in a tube with 50 mL of the above medium with shaking at 110 rpm at 37 °C. Then, 2 mL of solution was collected for analysis at predetermined time points and replaced with an equivalent volume of fresh medium. The amount of released dexamethasone was analyzed using the HPLC method and the amount of released bevacizumab was analyzed using the BCA assays described above.

Apoptosis Induction

To examine the apoptotic effect of the eBev-DPPNs or the cBev-DPNs, flow cytometric assays were performed. HUVECs were plated in 6-well plates and treated with drug suspended in serum-free medium after 12 h of starvation. HUVECs were washed and resuspended in PBS. Then, 50,000–100,000 HUVECs were collected and stained with Annexin V-fluorescein isothiocyanate (FITC) and propidium iodide (PI). Cell apoptosis was analyzed using a flow cytometer (EPICS XL/XL-MCL, Beckman Coulter, USA).

Wound Healing Assay

Would healing assays were performed as previously described[26] HUVECs were plated in 12-well plates. After the cells were allowed to have overgrown, a wound was scratched using a micropipette tip. Fresh M199 containing dexamethasone (10 μg/mL), bevacizumab (85 μg/mL), and eBev-DPPNs (containing dexamethasone 10 μg/mL) or cBev-DPNs (containing dexamethasone 10 μg/mL) was then added and co-incubated for 12 h, with M199 serving as a control. Finally, images were taken with an optical microscope (CKX41, Olympus, Japan) at a magnification of 10×. Migrated cells were manually counted, and the inhibition percentage was calculated based on the M199-treated cells as 100%.

Transwell Invasion Assay

Invasion of HUVECs in vitro was measured on Matrigel-coated (300 μg/mL) Transwell inserts with 8 μm pore size (BD, MA, USA). Cells were plated in the upper compartment at a density of 4×10^4 cells per well, and 100 μL medium containing dexamethasone (10 μg/mL), bevacizumab (85 μg/mL), and eBev-DPPNs (containing dexamethasone 10 μg/mL) or cBev-DPNs (containing dexamethasone 10 μg/mL) was added. $VEGF_{165}$ (10 ng/mL) was placed in the bottom compartment. After 24h of co-incubated of, cells that had invaded through the membrane were fixed and stained using Crystal violet solution and counted using a microscopy at a magnification of 20×.

Tube Formation Assay

Tube formation assays were performed to investigate the effect of the drugs on preventing formation of tube-like structures in vitro. For the tube formation assays, 24-well plates were coated with 300 μL Matrigel (8.6 mg/mL), and HUVECs at a density of 4×10^4 cells per well were seeded on Matrigel. Dexamethasone (10 μg/mL), bevacizumab (85 μg/mL), and eBev-DPPNs (containing dexamethasone 10 μg/mL) or cBev-DPNs (containing dexamethasone 10 μg/mL) were added immediately. After 6 h of incubation, the number of tube-like structures was counted and photoed using a microscope at a magnification of 20×.

VEGF Secretion Of HUVECs

To quantify VEGF production in HUVECs after treatment with nanoparticles, HUVECs were planted in a 96-well plate at a density of 5×10^4 cells per well. Hypoxia was induced with 200 μmol/L $CoCl_2$ and cell were then incubated with drugs in serum-free media at 37 °C for 72 h. At various time points, media was collected and centrifuged. The amount of VEGF protein in cell media was measured using commercially available Human VEGF ELISA kits, in accordance with manufacturer's instructions.

CAM Assay

The effect of the nanoparticles on angiogenesis in vivo was assessed using CAM assays. Briefly, fertilized chicken eggs were incubated at 37 °C with 60–70% relative humidity. On the seventh day of embryonic development, the eggs were sterilized with ethanol and opened (diameter ~10 mm) in the air chamber. The drug (dexamethasone, bevacizumab, and eBev-DPPNs or cBev-DPNs) solution in saline was gently added into each CAM. The entire process was performed under sterilized conditions. On the day 5 of incubation, CAMs were fixed in 3.7% formaldehyde and imaged. The number of blood vessels surrounding the administration area was counted in each CAM. The number of blood vessels in the control group without any drug was calculated as 100%.

Animal Studies

The laser-induced CNV model was established as previously described.[27,28] The chinchillaf rabbits were anesthetized via a subcutaneous injection of 10% chloral hydrate (3.5 mL/kg body weight), and following with the separate administration of Alcaine® and Mydriacyl® (both Alcon Laboratories Ltd., Fort Worth, TX, USA) to the right eyes of the rabbits for topical anesthesia and mydriasis, respectively. Nd: YAG laser irradiation (532 nm; Iris Radiation Systems, USA) was delivered through a Haag-Streit 900 slit lamp (Bern, Switzerland) with a piece of slide filled with 1 drop of Levofloxacin eye drops applied to the rabbits cornea of right eyes, the fellow eye was the control. Lesions were created with laser parameters that included 50 μm spot size, 0.1 s duration, and 0.7 W. The CNV lesions were studied at 28 days after laser photocoagulation by fluorescein fundus angiography (FFA) with a digital fundus camera (Heidelberg HRA-II, Germany). A mixture of 0.2 mL 10% fluorescein sodium with 1mL saline was injected into the Ear marginal vein of the rabbits. Late-phase angiograms were obtained 1 ~ 10 min after injection.

Briefly, the CNV model rabbits were divided into five groups of 3 rabbits each. The drug (dexamethasone, bevacizumab, and eBev-DPPNs or cBev-DPNs) solution in saline were intravitreally injected with 27-needle. After 28 days of treatment, FFA was performed again to detect vascular abnormality. The intensity of CNV area (laser spots was analyzed using ImageJ software (version 1.44p; National Institutes of Health, USA) and normalized against the total intensity of the entire viewing field.

Statistical Analysis

All results and measurements were expressed as the means ± SD. One-way analyses of variance were used to analyze statistically significant differences among treatment groups. P values of < 0.05 was considered statistically significant.

Results

Preparation Of Nanoparticles

Dexamethasone, a glucocorticoid hormone widely used to treat ophthalmic diseases, was loaded in the polymeric drug carrier to form DPPNs. Bevacizumab was used as a VEGF aptamer. PLGA was chosen as polymeric drug carrier. However, because nanoparticles made with only PLGA have a negative charge. PEI was added to adjust the zeta potential of nanoparticles for better electrostatic conjugation to bevacizumab. Particle size, PDI, surface charge, and bevacizumab binding efficiency of the different formulations of nanoparticles are shown in Tables 1 and 2. As seen in Table 1, the size of the DPPNs increased significantly, from 140 to 190nm, with the increase of PEI in the W phase from 0% to 0.8% (w/v). This was accompanied by an increase of the surface charge from -3 to 28 mV. The bevacizumab binding efficiency increased as the PEI content increased, at the same time, the diameter of the eBev-DPPNs increased from 189 to 222 nm. Accordingly, batch 5 was selected for further investigation due to desirable size and the zeta potential.

The ratio of bevacizumab and DPPNs affected the ability of the DPPNs to bind bevacizumab. As shown in Table 2, the ratios of bevacizumab and DPPNs were designed to be 1:2, 3:4, 1:1, 5:4, and 3:2. At high bevacizumab to DPPNs ratios, bevacizumab could not entirely conjugate with the DPPNs and free bevacizumab was observed. However, the amount of free bevacizumab decreased with decreasing bevacizumab to DPPNs ratios. At a bevacizumab to DPPNs ratio of 1:2, the binding efficiency was improved but the amount of reacted

Table 1 Optimization Of PEI Ratio In W Phase On eBev-DPPNs

Batch	Ratio Of PEI In W Phase (w/v, %)	DPPNs			eBev-DPPNs			BE (%)
		Size (d.nm)	PDI	Zeta Potential (mV)	Size (d.nm)	PDI	Zeta Potential (mV)	
1	0	146.0 ± 1.3	0.093 ± 0.036	−3.61 ± 0.90	-	-	-	-
2	0.3	154.4 ± 2.5	0.146 ± 0.090	13.42 ± 1.62	189.9 ± 5.4	0.256 ± 0.057	0.36 ± 0.89	44.21 ± 0.46
3	0.4	155.7 ± 3.3	0.131 ± 0.077	19.47 ± 2.89	190.4 ± 3.9	0.290 ± 0.066	−0.16 ± 0.55	66.30 ± 2.01
4	0.5	162.8 ± 3.0	0.162 ± 0.089	23.25 ± 1.87	207.4 ± 6.2	0.236 ± 0.038	1.06 ± 0.25	78.95 ± 2.57
5	0.6	175.0 ± 2.8	0.121 ± 0.033	28.20 ± 2.03	217.7 ± 5.3	0.279 ± 0.049	0.85 ± 0.37	85.64 ± 0.28
6	0.7	184.2 ± 1.9	0.032 ± 0.014	26.76 ± 3.27	221.0 ± 8.4	0.257 ± 0.033	−0.15 ± 0.89	82.98 ± 1.28
7	0.8	190.3 ± 5.7	0.168 ± 0.021	26.21 ± 3.45	222.7 ± 9.2	0.293 ± 0.067	0.33 ± 0.61	86.46 ± 1.38

Notes: The eBev-DPPNs are fabricated at DPPNs to bevacizumab at a ratio of 1:1. Binding efficiency is defined as percentage of the amount of reacted bevacizumab on the amount of bevacizumab used during the preparation process. Data are expressed as mean ± SD, n = 3.
Abbreviations: PEI, Polyethylenimine; DPPNs, dexamethasone-loading PLGA/PEI nanoparticles; eBev-DPPNs, electrostatically-conjugated bevacizumab-bearing DPPNs; PDI, polydispersity index; BE, binding efficiency.

Table 2 Optimization Of The Ratio Of DPPNs And Bevacizumab On eBev-DPPNs

Batch	Bevcizumab-to-DPPNs (w/w)	eBev-DPPNs			BE (%)
		Size (d.nm)	PDI	Zeta Potential (mV)	
8	1:2	193.8 ± 8.2	0.341 ± 0.081	0.86 ± 1.13	90.70 ± 1.59
9	3:4	215.6 ± 5.7	0.249 ± 0.037	0.89 ± 0.72	89.35 ± 1.81
10	1:1	217.7 ± 5.3	0.279 ± 0.049	0.85 ± 0.37	85.64 ± 0.28
11	5:4	248.2 ± 2.1	0.032 ± 0.045	0.44 ± 0.63	63.28 ± 0.73
12	3:2	253.3 ± 3.7	0.327 ± 0.019	0.51 ± 0.28	50.08 ± 0.55

Notes: The eBev-DPPNs are fabricated at 0.6% PEI ratio in W phase. Binding efficiency is defined as percentage of the amount of reacted bevacizumab on the amount of bevacizumab used during the preparation process. Data are expressed as mean ± SD, n = 3.
Abbreviations: DPPNs, dexamethasone-loading PLGA/PEI nanoparticles; eBev-DPPNs, electrostatically-conjugated bevacizumab-bearing DPPNs; PDI, polydispersity index; BE, binding efficiency.

bevacizumab was low. Therefore, a bevacizumab to DPPN ratio of 1:1 was selected to further investigations.

Characterization Of Nanoparticles

The DPNs, DPPNs, eBev-DPPNs and cBev-DPNs were prepared according to the selected optimized fabricate. Particle size, PDI, zeta potential and DL(%), EE(%), BE (%) of the eBev-DPPNs and cBev-DPNs was showed in Table 3. DLS and SEM images of the eBev-DPPNs and the cBev-DPNs are shown in Figure 1. The eBev-DPPNs and the cBev-DPNs were spherical in shape without aggregation. The diameter of nanoparticles observed in SEM images was consistent with the size measured by DLS analysis.

Stability Of Nanoparticles

To determine nanoparticle stability, the eBev-DPPNs and cBev-DPNs were suspended in PBS (20 mM, pH 7.4) and

Table 3 Characteristics Of The Optimized Formulations

Formulation	Size (d.nm)	PDI	Zeta Potential (mV)	DL (%)	EE (%)	BE (%)
DPNs	146.0 ± 1.3	0.093 ± 0.036	−3.61 ± 0.90	10.87 ± 0.96	65.21 ± 5.81	–
DPPNs	175.0 ± 2.8	0.121 ± 0.033	28.20 ± 2.03	11.14 ± 0.62	66.88 ± 3.62	–
eBev-DPPNs	217.7 ± 5.3	0.279 ± 0.049	0.85 ± 0.37	9.50 ± 0.30	56.97 ± 1.93	85.64 ± 0.28
cBev-DPNs	201.3 ±7.2	0.318 ± 0.084	0.31 ± 1.15	9.34 ± 0.07	56.01 ± 0.33	81.75 ± 2.12

Note: Data are expressed as mean ± SD, n = 3.
Abbreviations: DPNs, dexamethasone-loading PLGA nanoparticles; DPPNs, dexamethasone-loading PLGA/PEI nanoparticles; eBev-DPPNs, electrostatically-conjugated bevacizumab-bearing DPPNs; cBev-DPNs, chemically-conjugated bevacizumab-bearing DPNs; PDI, polydispersity index; PDI, polydispersity index; DL, drug loading; EE, encapsulation efficiency; BE, binding efficiency.

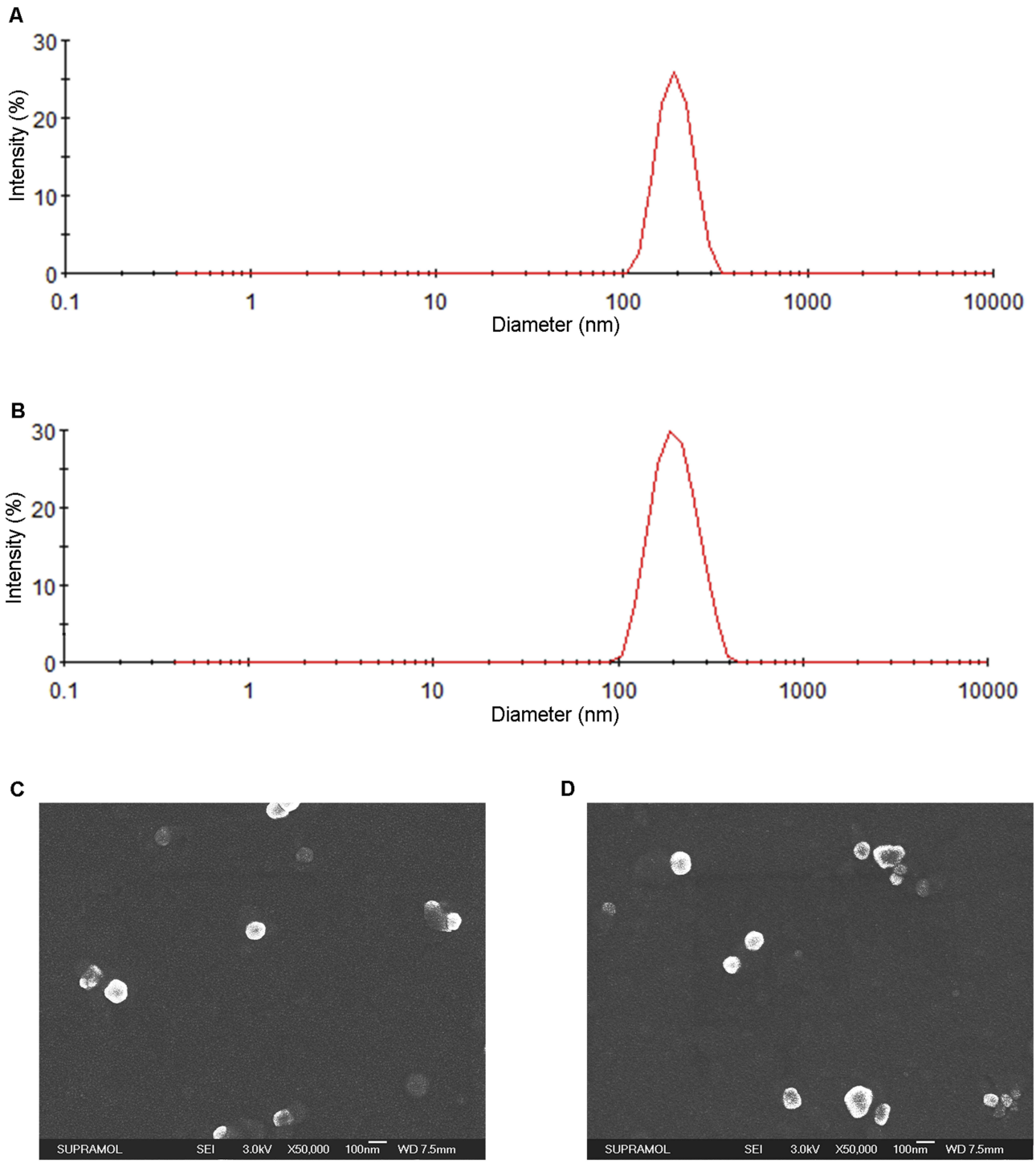

Figure 1 Characteristics of the eBev-DPPNs and cBev-DPNs. (**A**) Size distribution of eBev-DPPNs based on DLS; (**B**) Size distribution of cBev-DPNs based on DLS; (**C**) SEM images of eBev-DPPNs; (**D**) SEM images of cBev-DPNs. Data are expressed as mean ± SD, n = 3.

Abbreviations: eBev-DPPNs, electrostatically-conjugated bevacizumab-bearing DPPNs; cBev-DPNs, chemically-conjugated bevacizumab-bearing DPNs; DLS, dynamic light scattering; SEM, scanning electron microscopy.

vitreous humor of rabbit eyes at 37 °C. The particle size, PDI, and binding efficiency of bevacizumab in PBS are shown in Figure 2A–C. These parameters did not change significantly in PBS over 72 h of incubation at 37 °C. However, the size of the eBev-DPPNs and cBev-DPNs initially increased then decreased during incubation in vitreous humor, as shown in Figure 2D. Proteins from vitreous humor such as collagen, fibrillin, and opticin[29]

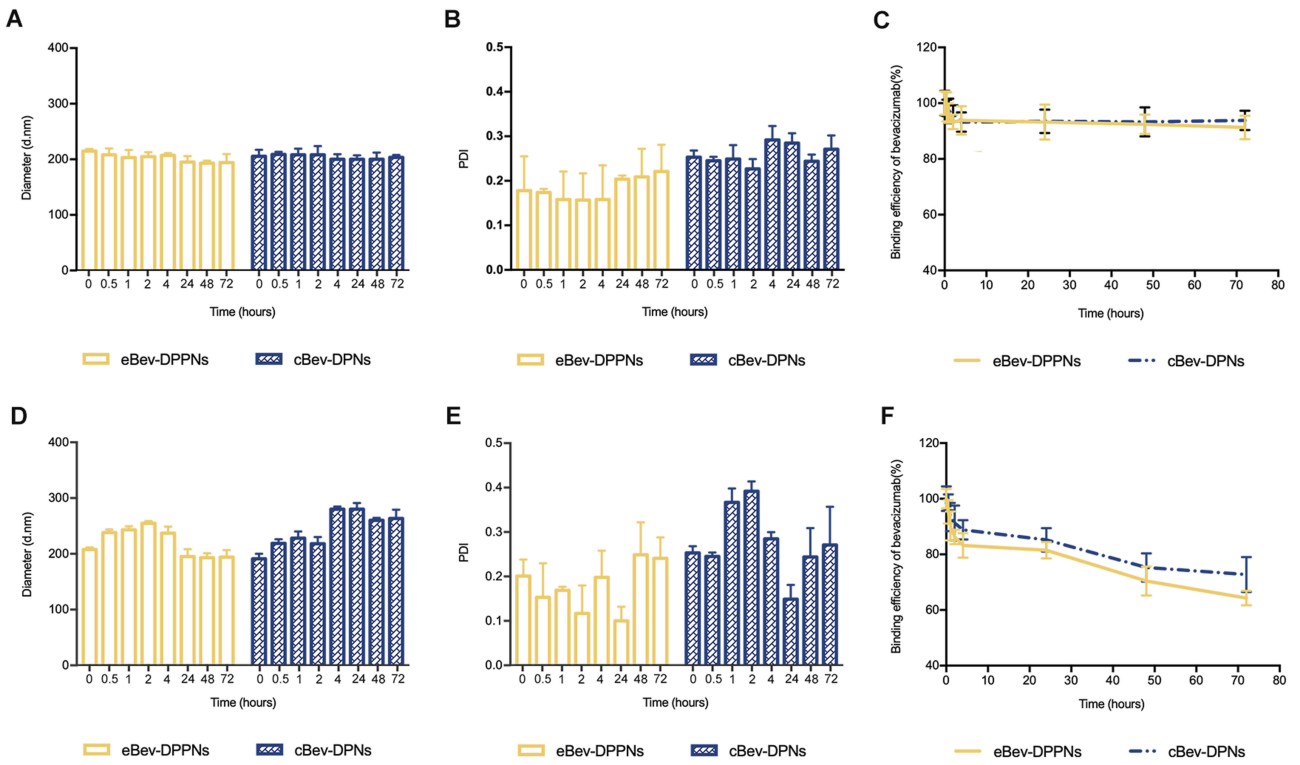

Figure 2 Stability of the eBev-DPPNs and cBev-DPNs. (**A**) Particle size; (**B**) PDI; (**C**) Binding efficiency of bevacizumab in PBS; (**D**) Particle size; (**E**) PDI; (**F**) Binding efficiency of bevacizumab in the vitreous humor of rabbit eyes. Data are expressed as mean ± SD, n = 3.
Abbreviations: eBev-DPPNs, electrostatically-conjugated bevacizumab-bearing DPPNs; cBev-DPNs, chemically-conjugated bevacizumab-bearing DPNs.

may have adsorbed to nanoparticles, leading to an increase in nanoparticles size. Over time, the interactions between cBev-DPNs and vitreous humor proteins may have become stronger, which could have caused the structures to become more compact with decreased sizes.[22] The cBev-DPNs may interact more strongly with bevacizumab than eBev-DPPNs, so that their sizes decreased more. As shown in Figure 2F, the binding efficiency of bevacizumab on both the eBev-DPPNs and the cBev-DPNs decreased.

Structural Stability Of The Bevacizumab From The Surface Of The Nanoparticles

The primary structural stability of bevacizumab, evaluated by SEC-HPLC, is shown in Figure 3A. Bevacizumab dissociated from eBev-DPPNs presented a peak corresponding to original bevacizumab in solution at 17.2 min. An extra broad peak appeared after 12 min in the bevacizumab from cBev-DPNs. The secondary and tertiary structural stability of bevacizumab was analyzed using CD (Figure 3B) and fluorescence spectroscopy (Figure 3C). Both the CD signal intensity of bevacizumab and the fluorescence intensity of bevacizumab dissociated from the eBev-DPPNs had more similarities compared to original bevacizumab solution than did bevacizumab dissociated from the cBev-DPNs.

In Vitro Release Study

The dexamethasone release behavior of the eBev-DPPNs and the cBev-DPNs, as shown in Figure 4A, was obtained in PBS (20 mM, pH 7.4) with 0.5% Tween-80 over 120 h. An initial burst of dexamethasone was released from the eBev-DPPNs and the cBev-DPNs, with 39.6% and 27.7% released within 12 h, respectively. At 120 h, the accumulated release of dexamethasone was 68.1% and 61.2% from the eBev-DPPNs and the cBev-DPNs, respectively

The bevacizumab release behavior of the eBev-DPPNs and the cBev-DPNs was shown in Figure 4B. An initial burst of dexamethasone was released from the eBev-DPPNs and the cBev-DPNs, with 25.2% and 13.5% released within 12 h, respectively. At 120 h, the accumulated release of bevacizumab was 60.2% and 31.4% from the eBev-DPPNs and the cBev-DPNs, respectively.

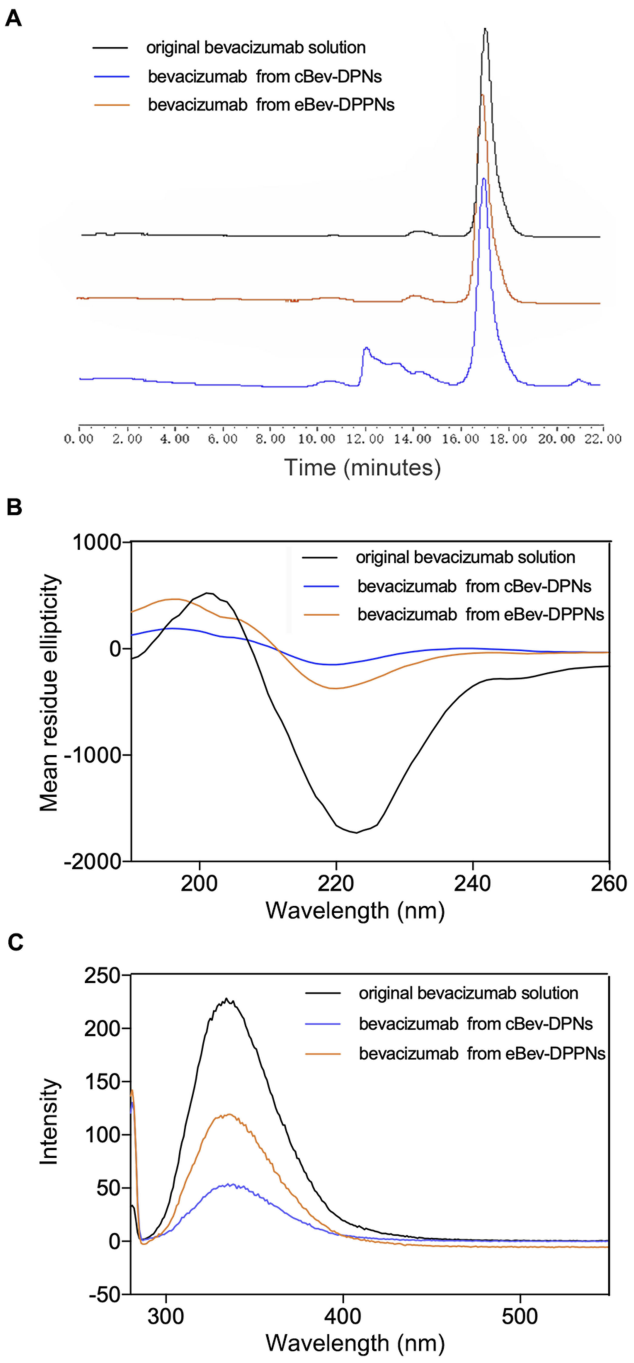

Figure 3 Structural stability of the bevacizumab on the surface of the eBev-DPPNs and cBev-DPNs.
Notes: (**A**) SEC-HPLC chromatograms; (**B**) CD spectra; (**C**) Fluorescence spectra.
Abbreviations: eBev-DPPNs, electrostatically-conjugated bevacizumab-bearing DPPNs; cBev-DPNs, chemically-conjugated bevacizumab-bearing DPNs.

Apoptosis Induction

The role of endothelial cell apoptosis is potentially important for the angiogenic process.[30,31] As shown in Figure 5, the percentage of live cells was 99.60%, 78.60%, 65.71%, 31.06%, and 37.08% in the untreated control group, dexamethasone-treated group, bevacizumab-treated group, eBev-DPPNs-treated group and cBev-DPNs-treated group, respectively. All treated groups could efficiently induce apoptosis in a large amount of HUVECs after 12 h of incubation. The eBev-DPPNs in particular induced the highest rate of apoptosis ratio.

Wound Healing Assay

The inhibitory activity of nanoparticles on cell migration was observed by wound healing assays. As shown in Figure 6, both bevacizumab and dexamethasone caused HUVECs migration to decrease, and a strong decrease in cell migration was observed after incubation with eBev-DPPNs and cBev-DPNs. The eBev-DPPNs induced a stronger inhibitory effect on cell migration than cBev-DPNs (9.3 ± 2.3% vs 15.03 ± 1.31%, $p < 0.05$).

Transwell Invasion Assay

Migration and invasion of endothelial cells are essential in vitro angiogenesis. Transwell invasion assays were conducted In the presence of bevacizumab, dexamethasone, eBev-DPPNs, or cBev-DPNs to evaluate the ability of HUVECs to pass through the Matrigel and Transwell membrane barrier. As shown in Figure 7, the invasion of endothelial cells was significantly more inhibited when cells were treated with eBev-DPPNs group than when treated with cBev-DPNs group (7.3 ± 1.30% vs 13.7 ± 2.60%, $p < 0.05$).

Tube Formation Assay

As an in vitro model of angiogenesis, HUVECs can organize into capillary-like structures in Matrigel. As shown in Figure 8, HUVECs formed a large amount of capillary-like structures within 6 h in the untreated control group. In contrast, HUVECs tube formation was inhibited significantly by treating with bevacizumab, dexamethasone, eBev-DPPNs, and cBev-DPNs. The number of capillary-like structures formed was quantified using an inverted microscope. The number of capillary-like structures was significantly reduced in cells treated with eBev-DPPNs compared with cells treated with cBev-DPNs ($p < 0.05$).

VEGF Secretion Of HUVECs

To confirm the inhibition of VEGF secretion by the nanoparticles, the amount of VEGF in the media was quantified after HUVEC incubation with bevacizumab, dexamethasone, eBev-DPPNs, and cBev-DPNs, as shown in Figure 9. $CoCl_2$ was used to induce hypoxia in HUVECs to promote VEGF secretion. After 24 h of co-incubation,

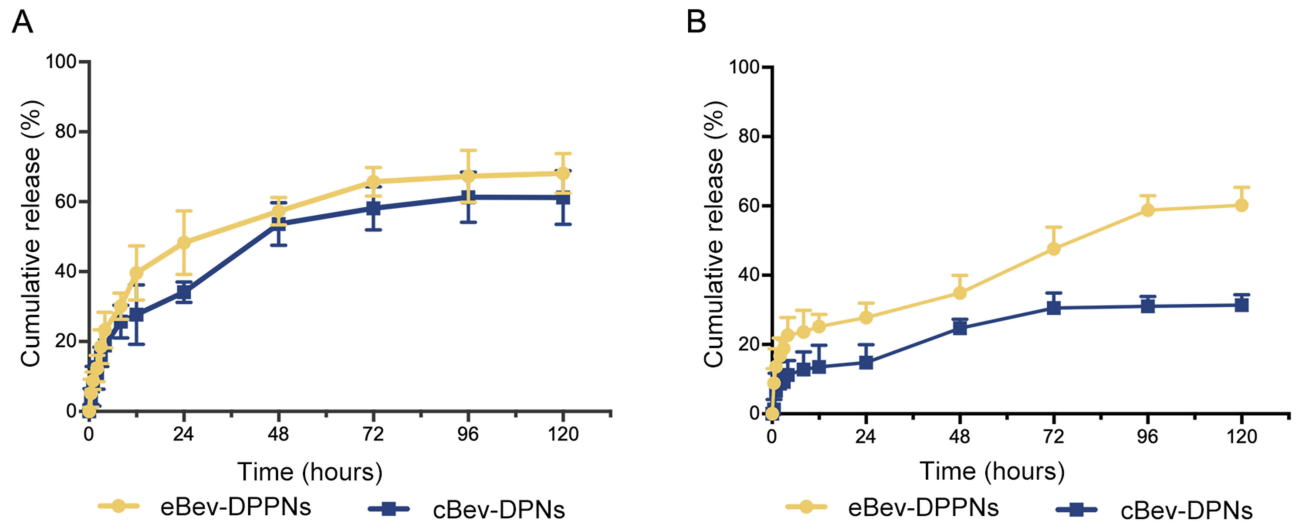

Figure 4 (**A**) In vitro release of dexamethasone from the eBev-DPPNs and cBev-DPNs; (**B**) In vitro release of bevacizumab from the eBev-DPPNs and cBev-DPNs. Data are expressed as mean ± SD, n = 3.
Abbreviations: eBev-DPPNs, electrostatically-conjugated bevacizumab-bearing DPPNs; cBev-DPNs, chemically-conjugated bevacizumab-bearing DPNs.

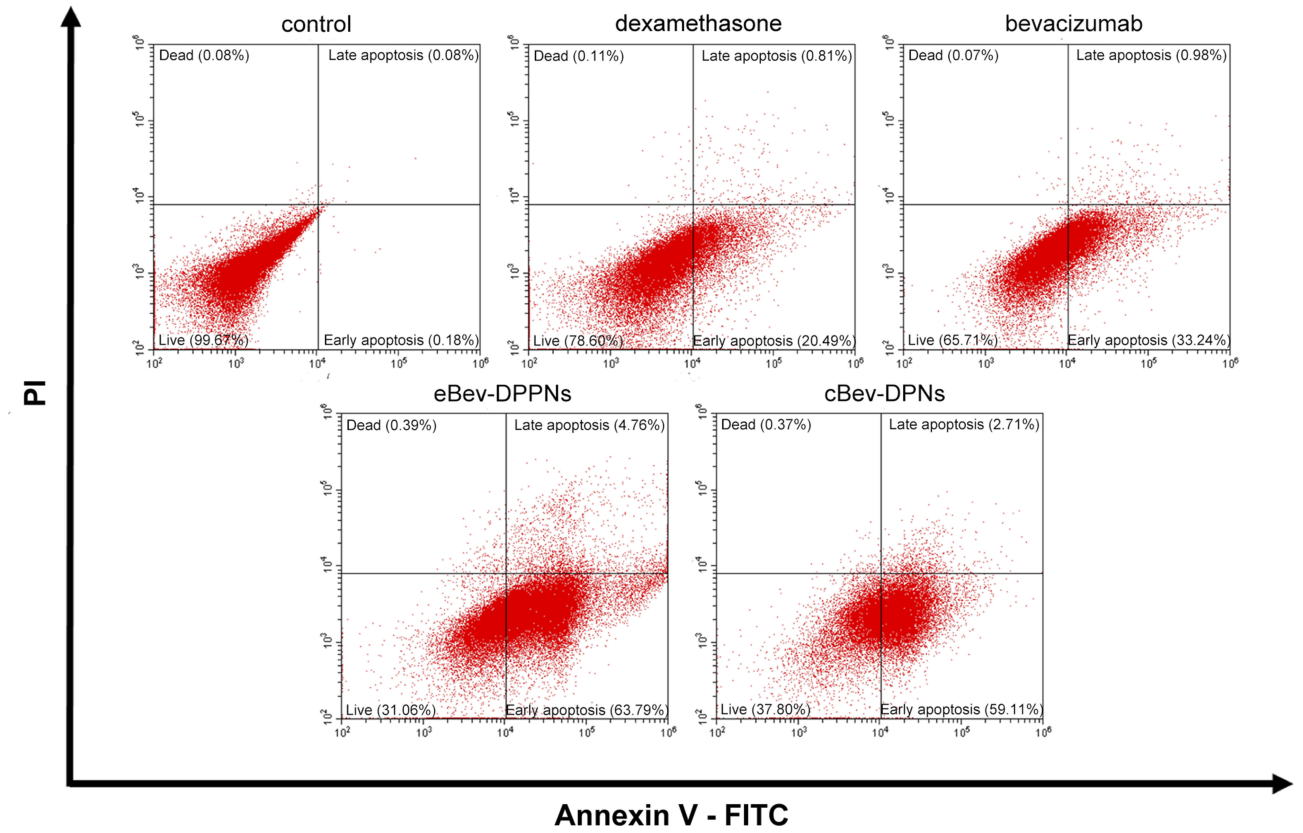

Figure 5 Induction of apoptosis by nanoparticles on HUVECs. Data are expressed as mean ± SD, n = 6.
Abbreviations: eBev-DPPNs, electrostatically-conjugated bevacizumab-bearing DPPNs; cBev-DPNs, chemically-conjugated bevacizumab-bearing DPNs; PI, propidium iodide.

bevacizumab, dexamethasone, eBev-DPPNs, and cBev-DPNs all caused VEGF secretion from HUVECs induced with $CoCl_2$ to decrease ($p < 0.05$). A stronger inhibitory effect on VEGF secretion from HUVECs was observed in cells treated with eBev-DPPNs compared with other groups after 48 h of co-incubation with $CoCl_2$ ($p < 0.05$).

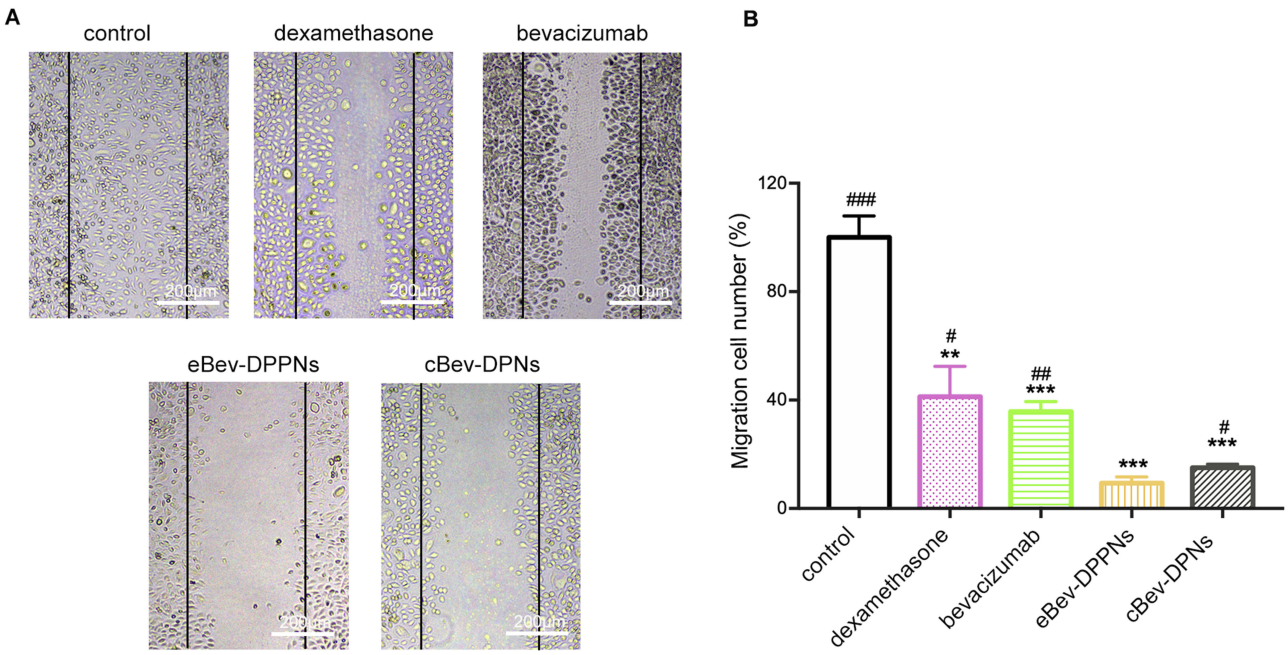

Figure 6 Migration inhibition by nanoparticles on HUVECs in wound healing assays. (**A**) Representative images of HUVECs migration; (**B**) Migration number of HUVECs. Data are expressed as mean ± SD, n = 6. **p < 0.01, ***p < 0.001 vs control; #p < 0.05, ##p < 0.01, ###p < 0.001 vs eBev-DPPNs.
Abbreviations: eBev-DPPNs, electrostatically-conjugated bevacizumab-bearing DPPNs; cBev-DPNs, chemically-conjugated bevacizumab-bearing DPNs.

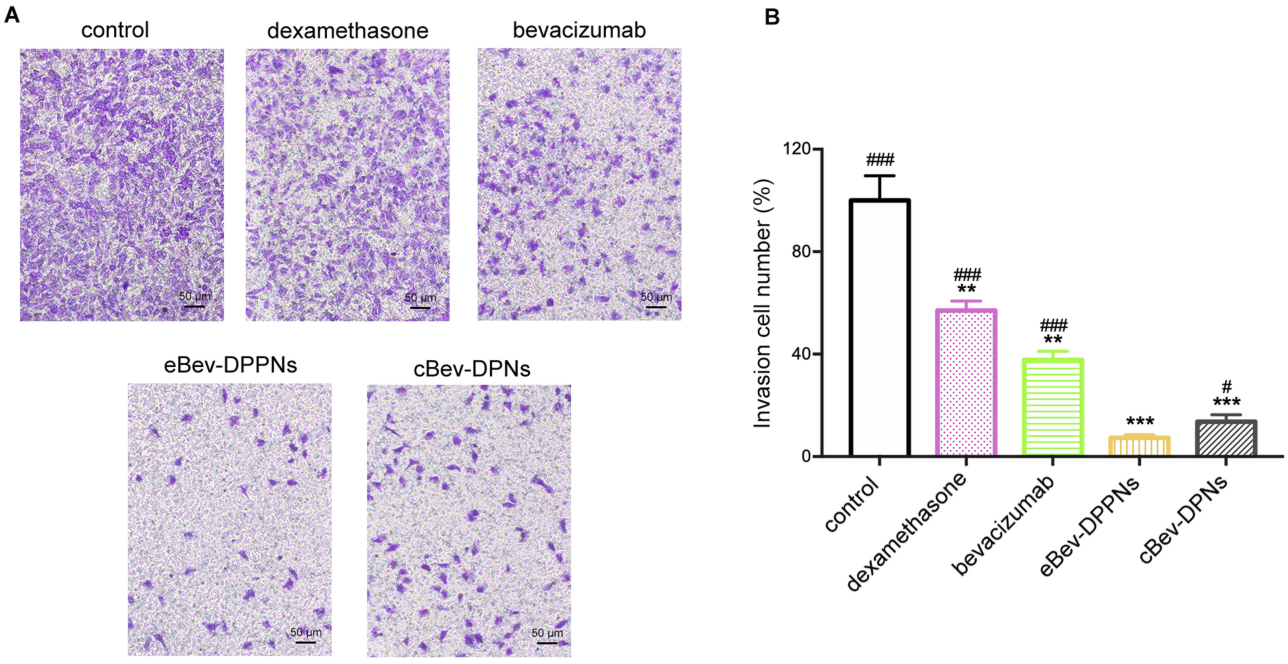

Figure 7 Invasion inhibition by nanoparticles on HUVECs in Transwell assays. (**A**) Representative images of HUVECs invasion; (**B**) Invasion number of HUVECs. Data are expressed as mean ± SD, n = 6. **p < 0.01, ***p < 0.001 vs control; #p < 0.05, ###p < 0.001 vs eBev-DPPNs.
Abbreviations: eBev-DPPNs, electrostatically-conjugated bevacizumab-bearing DPPNs; cBev-DPNs, chemically-conjugated bevacizumab-bearing DPNs.

Cam

The in vivo anti-angiogenic effects of treatments were tested on embryonic tissues. Notably, drugs inhibited the growth of new blood vessels and thus significantly reduced vascular density (Figure 10). The eBev-DPPNs reduced the percentages of blood vessels relative to the blood vessels in the negative control to as low as 4.43%, significantly less than bevacizumab or dexamethasone

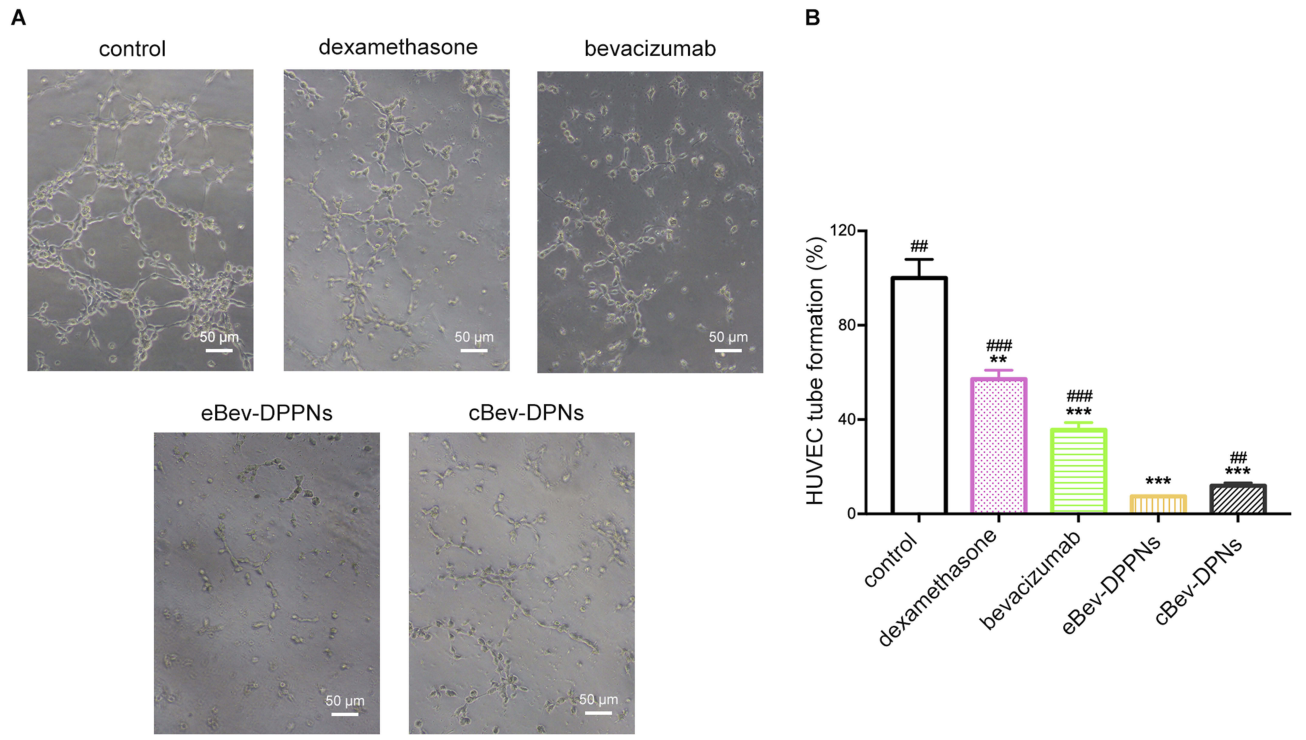

Figure 8 Tube formation inhibition by nanoparticles on HUVECs. (**A**) Representative images of HUVECs tube formation; (**B**) Tube formation capacity of HUVECs. Data are expressed as mean ± SD, n = 6. **p < 0.01, ***p < 0.001 vs control; ##p < 0.01, ###p < 0.001 vs eBev-DPPNs.
Abbreviations: eBev-DPPNs, electrostatically-conjugated bevacizumab-bearing DPPNs; cBev-DPNs, chemically-conjugated bevacizumab-bearing DPNs.

treatment ($p < 0.01$) and even treatment with cBev-DPNs ($p < 0.05$).

Animal Studies

To confirm the role of the eBev-DPPNs for potential intravitreal applications, a rabbit CNV model was constructed by laser photocoagulation. The eBev-DPPNs intravitreal injection was applied in the rabbit CNV model. FFA (Figure 11) showed that the leakage area of CNV decreased in the eBev-DPPNs and cBev-DPNs groups significantly ($p < 0.001$).

Discussion

Nanoparticles have been widely used as carriers for drug delivery over the past decades. Here, the biocompatible, biodegradable polymer PLGA was used to encapsulate dexamethasone in nanoparticles, then the nanoparticles were conjugated with bevacizumab for intravitreal anti-angiogenic therapy.

Particle size is important for intravitreal applications. The diameters of both the eBev-DPPNs and cBev-DPNs were about 200 nm. Sakurai et al demonstrated that nanospheres with a diameter of about 200 nm were observed in the retina and in other ocular posterior segment tissues, while nanospheres with a diameter of 2 μm were seen in the vitreous cavity and trabecular meshwork.[32]

Stability is also important for nanoparticle storage and medical applications.[33] The stability of the eBev-DPPNs and the cBev-DPNs in PBS or vitreous humor of rabbit eyes at 37 °C was evaluated. Figure 2D–F showed that particle size, PDI, and bevacizumab binding efficiency showed little change over 72 h. These results indicated that bevacizumab had been released from the surface of nanoparticles into the vitreous humor to exert its effects.

The structural stability and biological activity of protein drugs are closely related. Bevacizumab was more integrated on the surface of the eBev-DPPNs than on the cBev-DPNs, indicating that the electrostatic conjugation strategy between dexamethasone-loaded nanoparticles and bevacizumab better maintained the structural stability of bevacizumab than the chemical conjugation strategy, possibly explaining why the eBev-DPPNs had better therapeutic efficacy than the cBev-DPNs.

The pH of vitreous humor is about 7.4, the in vitro release behavior of dexamethasone from eBev-DPPNs and cBev-DPNs was tested in media with pH 7.4 and incubated at 37 °C. The eBev-DPPNs released dexamethasone

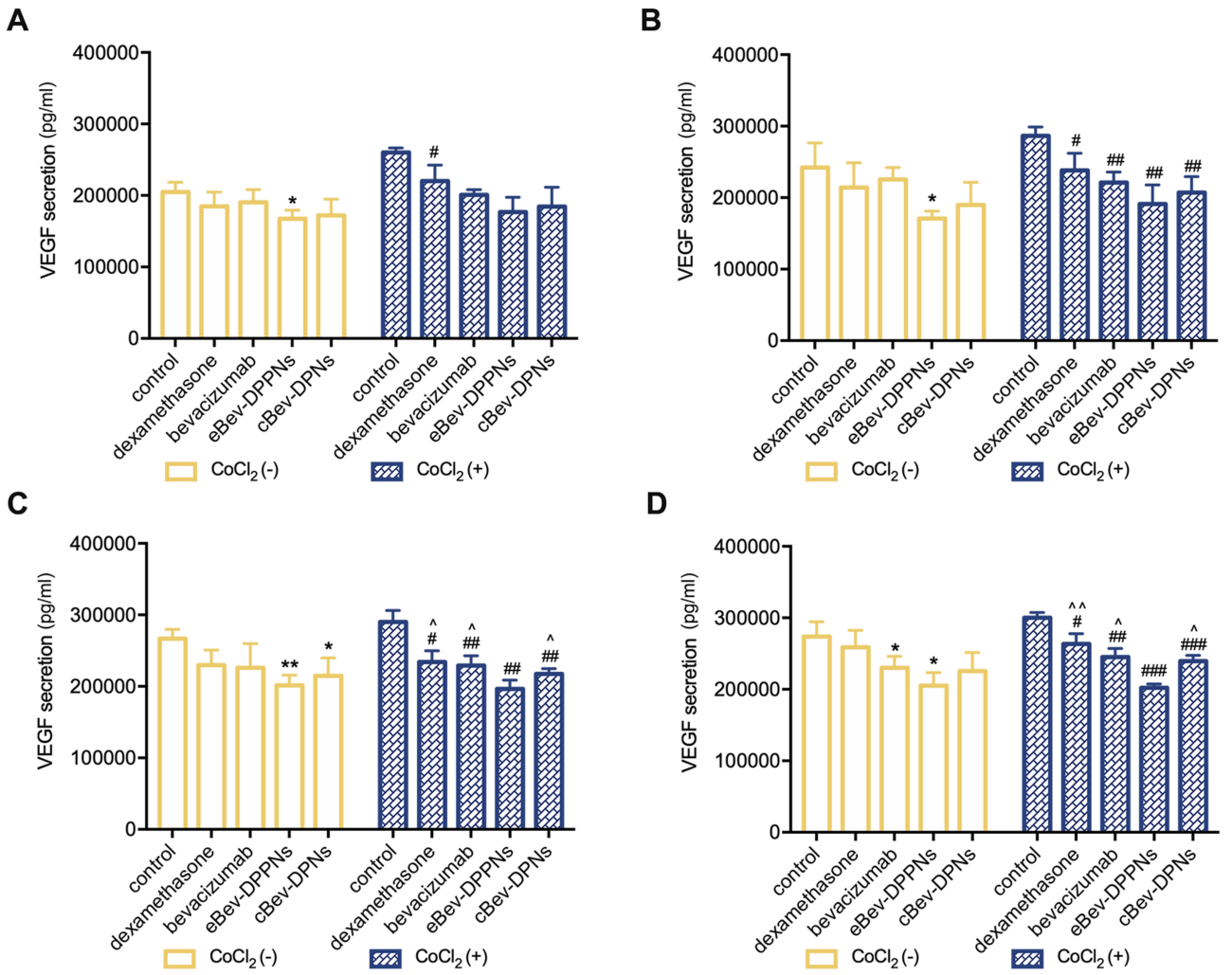

Figure 9 VEGF secretion inhibition by nanoparticles on HUVECs. (**A**) VEGF secretion at 12 h; (**B**) VEGF secretion at 24 h; (**C**) VEGF secretion at 48 h; (**D**) VEGF secretion at 72 h. Data are expressed as mean ± SD, n = 6. *p < 0.05, **p < 0.01 vs control without $CoCl_2$; #p < 0.05, ##p < 0.01, ###p < 0.001 vs control with $CoCl_2$; ^p < 0.05, ^^p < 0.01 vs eBev-DPPNs with $CoCl_2$.

Abbreviations: VEGF, vascular endothelial growth factor; eBev-DPPNs, electrostatically-conjugated bevacizumab-bearing DPPNs; cBev-DPNs, chemically-conjugated bevacizumab-bearing DPNs.

slightly faster than the cBev-DPNs. This result might be due to the fact that bevacizumab dissociated more slowly from the surface of the cBev-DPNs than from the eBev-DPPNs, as shown in Figure 4B. The eBev-DPPNs released dexamethasone visibly faster than the cBev-DPNs. This result might be due to the fragility of electrostatic bonding in the eBev-DPPNs that affected by physiological salt in the release conditions and the degradation of the nanoparticles. The faster dexamethasone release and bevacizumab release of eBev-DPPNs provides a key advantage, benefitting treatment by allowing the therapeutic window to be reached faster.

The eBev-DPPNs have demonstrated efficacy in a series of angiogenic processes, including apoptosis, migration, invasion, and tube formation. These results suggest that combined treatment with dexamethasone and bevacizumab had improved anti-angiogenic effects on HUVECs than treatment with dexamethasone or bevacizumab alone. The eBev-DPPNs showed stronger inhibitory effects than cBev-DPNs. It has been verified that high VEGF expression can be detected in HUVECs induced with $CoCl_2$. VEGF as a pro-angiogenic factor plays a significant role in the migration, invasion, and tube formation of endothelial cells, which are all required for angiogenesis.[34,35] The eBev-DPPNs also strongly inhibited VEGF secretion from HUVECs induced by $CoCl_2$. CAM is widely used to study the angiogenic or anti-angiogenic activities of drugs in vivo. The present data showed that eBev-DPPNs were more efficient than other treatments. This finding was consistent with the in vitro anti-angiogenesis assays on

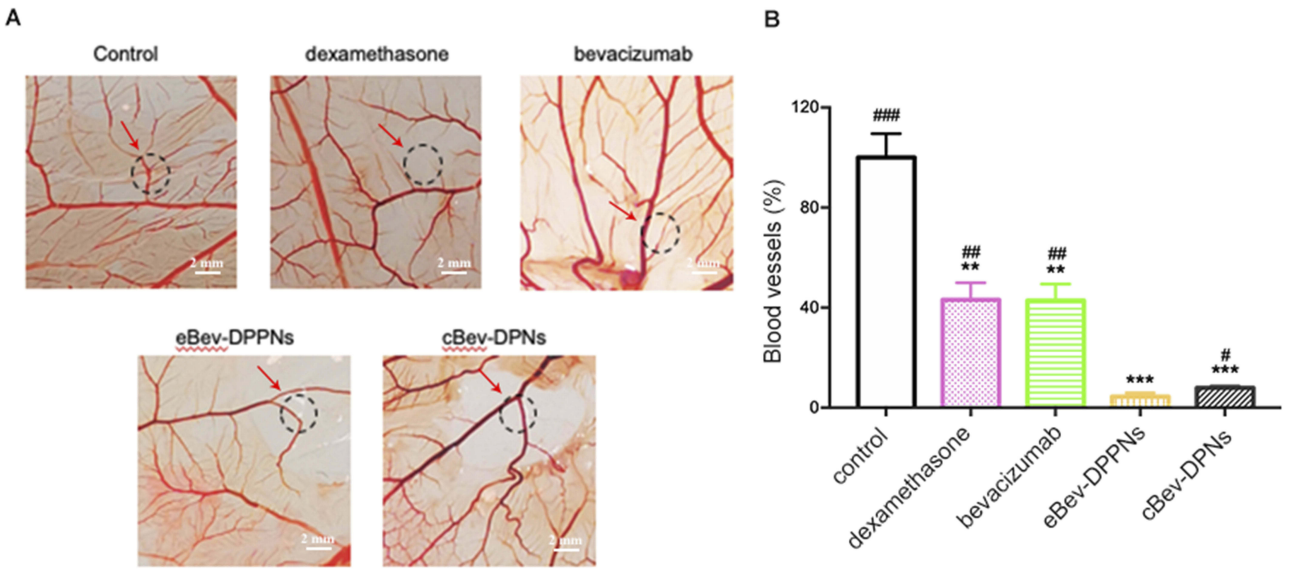

Figure 10 Anti-angiogenesis effects in vivo on chorioallantoic membranes. (**A**) Representative images of angiogenesis; (**B**) The amount of blood vessel on chorioallantoic membranes. Data are expressed as mean ± SD, n = 10. **p < 0.01, ***p < 0.001 vs control; #p < 0.05, ##p < 0.01, ###p < 0.001 vs eBev-DPPNs.
Abbreviations: eBev-DPPNs, electrostatically-conjugated bevacizumab-bearing DPPNs; cBev-DPNs, chemically-conjugated bevacizumab-bearing DPNs.

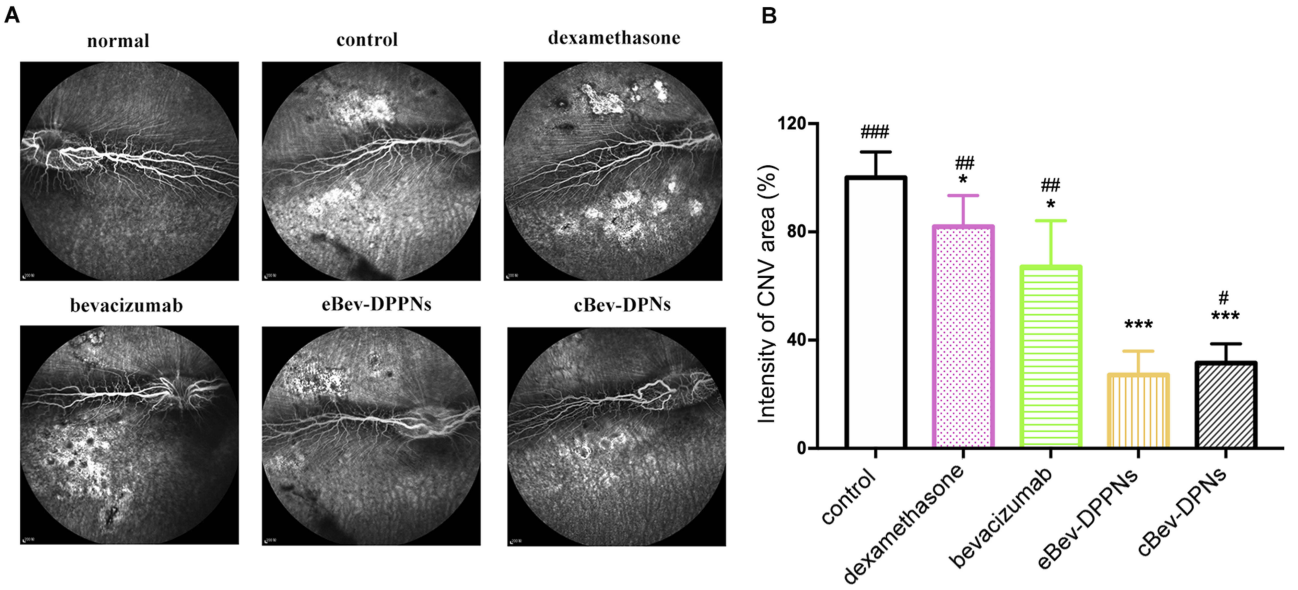

Figure 11 The inhibition of CNV area on laser-induced CNV rabbits model. (**A**) Representative images of the leakage area of CNV; (**B**) The intensity of CNV area on rabbits fundus. Data are expressed as mean ± SD, n = 3. *p < 0.05, ***p < 0.001 vs control; #p < 0.05, ##p < 0.01, ###p < 0.001 vs eBev-DPPNs.
Abbreviations: eBev-DPPNs, electrostatically-conjugated bevacizumab-bearing DPPNs; cBev-DPNs, chemically-conjugated bevacizumab-bearing DPN; CNV, Choroidal neovascularization.

HUVECs described above. These results confirmed that eBev-DPPNs had excellent anti-angiogenic effects, likely due to their abilities to quickly release dexamethasone (Figure 4), and to maintain the structural stability of bevacizumab (Figure 3). These nanoparticles have great promise for intravitreal applications, including treatment of AMD.

In brief, angiogenesis plays a critical role in AMD and VEGF is among the most important cytokines in angiogenesis.[36] Dexamethasone can interfere with VEGF expression or action,[8] while bevacizumab can target and combine with VEGF.[10] In the present study, the eBev-DPPNs could increase anti-angiogenic efficacy compared with treatment with dexamethasone or bevacizumab alone

and even compared with cBev-DPNs. Moreover, the eBev-DPPNs had increased CNV inhibition efficacy compared with treatment with dexamethasone or bevacizumab alone and also compared with cBev-DPNs. The eBev-DPPNs merit future investigation to validate and improve their clinical use in treating AMD and other angiogenesis-dependent diseases.

Conclusion

The eBev-DPPNs were prepared through electrostatic interactions between positively charged PEI and negatively charged bevacizumab. The eBev-DPPNs were smooth spheres and had small size with narrow size distribution. Apoptosis, migration, invasion, and tube formation assays demonstrated that the eBev-DPPNs had significant anti-angiogenic effects on HUVECs. The eBev-DPPNs also provided a strong inhibitory effect on VEGF secretion from HUVECs. Moreover, in vivo CAM assays showed eBev-DPPNs dramatically reduced the amount of blood vessels formed. Animal studies showed eBev-DPPNs decreased the leakage area of CNV on rabbit CNV model. In conclusion, these results indicate that the eBev-DPPNs have great promise as a novel therapeutic for anti-angiogenic treatment.

Acknowledgement

This research was supported by the Jilin Province Science and Technology Development Program (No. 20180101269JC), and the State Key Laboratory of Long-Acting and Targeting Drug Delivery System, and Shandong Luye Pharmaceutical Co., Ltd.

Disclosure

The authors report no conflicts of interest in this work.

References

1. Zhao M, Mantel I, Gelize E, et al. Mineralocorticoid receptor antagonism limits experimental choroidal neovascularization and structural changes associated with neovascular age-related macular degeneration. *Nat Commun*. 2019;10:1–13. doi:10.1038/S41467-018-08125-6
2. Mu H, Wang Y, Chu Y, et al. Multivesicular liposomes for sustained release of bevacizumab in treating laser-induced choroidal neovascularization. *Drug Deliv*. 2018;25(1):1372–1383. doi:10.1080/10717544.2018.1474967
3. Ambati J, Ambati BK, Yoo SH, Ianchulev S, Adamis AP. Age-related macular degeneration: etiology, pathogenesis, and therapeutic strategies. *Surv Ophthalmol*. 2003;48(3):257–293. doi:10.1016/S0039-6257(03)00030-4
4. Iyer S, Radwan AE, Hafezi-Moghadam A, Malyala P, Amiji M. Long-acting intraocular delivery strategies for biological therapy of age-related macular degeneration. *J Control Release*. 2019;296:140–149. doi:10.1016/j.jconrel.2019.01.007
5. Papadopoulos N, Martin J, Ruan Q, et al. Binding and neutralization of vascular endothelial growth factor (VEGF) and related ligands by VEGF Trap, ranibizumab and bevacizumab. *Angiogenesis*. 2012;15(2):171–185. doi:10.1007/s10456-011-9249-6
6. Brown DM, Kaiser PK, Michels M, et al. Ranibizumab versus verteporfin for neovascular age-related macular degeneration. *N Engl J Med*. 2006;355(14):1432–1444. doi:10.1056/NEJMoa062655
7. Krzystolik MG, Afshari MA, Adamis AP, et al. Prevention of experimental choroidal neovascularization with intravitreal anti-vascular endothelial growth factor antibody fragment. *Arch Ophthalmol*. 2002;120(3):338–346. doi:10.1001/archopht.120.3.338
8. Michels S, Rosenfeld PJ, Puliafito CA, Marcus EN, Venkatraman AS. Systemic bevacizumab (Avastin) therapy for neovascular age-related macular degeneration: twelve-week results of an uncontrolled open-label clinical study. *Ophthalmology*. 2005;112(6):1035–1047.e1039. doi:10.1016/j.ophtha.2005.02.007
9. Hoffart L, Matonti F, Conrath J, et al. Inhibition of corneal neovascularization after alkali burn: comparison of different doses of bevacizumab in monotherapy or associated with dexamethasone. *Clin Experiment Ophthalmol*. 2010;38(4):346–352. doi:10.1111/ceo.2010.38.issue-4
10. Nauck M, Karakiulakis G, Perruchoud AP, Papakonstantinou E, Roth M. Corticosteroids inhibit the expression of the vascular endothelial growth factor gene in human vascular smooth muscle cells. *Eur J Pharmacol*. 1998;341(2–3):309–315. doi:10.1016/S0014-2999(97)01464-7
11. Hiroshi T, Kazuaki M, Junichi K, et al. Intravitreal injection of corticosteroid attenuates leukostasis and vascular leakage in experimental diabetic retina. *Invest Ophthalmol Vis Sci*. 2005;46(4):1440–1444.
12. Zhang L, Chan JM, Gu FX, et al. Self-assembled lipid–polymer hybrid nanoparticles: a robust drug delivery platform. *ACS Nano*. 2008;2(8):1696–1702. doi:10.1021/nn800275r
13. Xie J, Yang Z, Zhou C, Zhu J, Lee RJ, Teng LJBA. Nanotechnology for the delivery of phytochemicals in cancer therapy. *Biotech Adv*. 2016;34(4):343–353.
14. Garg NK, Singh B, Sharma G, et al. Development and characterization of single step self-assembled lipid polymer hybrid nanoparticles for effective delivery of methotrexate. *RSC Adv*. 2015;5(77):62989–62999. doi:10.1039/C5RA12459J
15. Gomez-Graete C, Tsapis N, Besnard M, Bochot A, Fattal E. Encapsulation of dexamethasone into biodegradable polymeric nanoparticles. *Int J Pharm*. 2007;331(2):153–159. doi:10.1016/j.ijpharm.2006.11.028
16. Barcia E, Herrero-Vanrell R, Diez A, Alvarez-Santiago C, Lopez I, Calonge M. Downregulation of endotoxin-induced uveitis by intravitreal injection of polylactic-glycolic acid (PLGA) microspheres loaded with dexamethasone. *Exp Eye Res*. 2009;89(2):238–245. doi:10.1016/j.exer.2009.03.012
17. Xu J, Wang Y, Li Y, et al. Inhibitory efficacy of intravitreal dexamethasone acetate-loaded PLGA nanoparticles on choroidal neovascularization in a laser-induced rat model. *J Ocul Pharmacol Ther*. 2007;23(6):527–539. doi:10.1089/jop.2007.0002
18. Shen J, Durairaj C, Lin T, Liu Y, Burke J. Ocular pharmacokinetics of intravitreally administered brimonidine and dexamethasone in animal models with and without blood-retinal barrier breakdown. *Invest Ophthalmol Vis Sci*. 2014;55(2):1056–1066. doi:10.1167/iovs.13-13650
19. Kassumeh SA, Wertheimer CM, von Studnitz A, et al. Poly(lactic-co-glycolic) acid as a slow-release drug-carrying matrix for methotrexate coated onto intraocular lenses to conquer posterior capsule opacification. *Curr Eye Res*. 2018;43(6):702–708. doi:10.1080/02713683.2018.1437455
20. Nimesh S. 10 - Polyethylenimine nanoparticles. In: Nimesh S, editor. *Gene Therapy*. Woodhead Publishing; 2013:197–223.
21. Olbrich C, Bakowsky U, Lehr C-M, Müller RH, Kneuer C. Cationic solid-lipid nanoparticles can efficiently bind and transfect plasmid DNA. *J Control Release*. 2001;77(3):345–355. doi:10.1016/S0168-3659(01)00506-5

22. Yu K, Zhao J, Zhang Z, et al. Enhanced delivery of Paclitaxel using electrostatically-conjugated Herceptin-bearing PEI/PLGA nanoparticles against HER-positive breast cancer cells. *Int J Pharm*. 2016;497(1–2):78–87. doi:10.1016/j.ijpharm.2015.11.033
23. Terelak-Borys B, Zagajewska K, Jankowska-Lech I, Tesla P, Grabska-Liberek I. Combined treatment in punctate inner choroidopathy. *Ther Clin Risk Manag*. 2016;12:1467–1471. doi:10.2147/TCRM.S110556
24. Fornaguera C, Dols-Perez A, Caldero G, Garcia-Celma MJ, Camarasa J, Solans C. PLGA nanoparticles prepared by nano-emulsion templating using low-energy methods as efficient nanocarriers for drug delivery across the blood-brain barrier. *J Control Release*. 2015;211:134–143. doi:10.1016/j.jconrel.2015.06.002
25. Liu J, Li S, Li G, et al. Highly bioactive, bevacizumab-loaded, sustained-release PLGA/PCADK microspheres for intravitreal therapy in ocular diseases. *Int J Pharm*. 2019;563:228–236. doi:10.1016/j.ijpharm.2019.04.012
26. Gong C, Deng S, Wu Q, et al. Improving antiangiogenesis and anti-tumor activity of curcumin by biodegradable polymeric micelles. *Biomaterials*. 2013;34(4):1413–1432. doi:10.1016/j.biomaterials.2012.10.068
27. Qi X, Cai J, Ruan Q, et al. γ-Secretase inhibition of murine choroidal neovascularization is associated with reduction of superoxide and proinflammatory cytokines. *Invest Ophthalmol Vis Sci*. 2012;53(2):574–585.
28. Liu L, Qi X, Chen Z, et al. Targeting the IRE1α/XBP1 and ATF6 arms of the unfolded protein response enhances VEGF blockade to prevent retinal and choroidal neovascularization. *Am J Pathol*. 2013;182(4):1412–1424. doi:10.1016/j.ajpath.2012.12.020
29. Bishop PN. Structural macromolecules and supramolecular organisation of the vitreous gel. *Prog Retin Eye Res*. 2000;19(3):323–344. doi:10.1016/S1350-9462(99)00016-6
30. Chan LW, Camphausen K. Angiogenic tumor markers, antiangiogenic agents and radiation therapy. *Expert Rev Anticancer Ther*. 2003;3(3):357–366. doi:10.1586/14737140.3.3.357
31. Li ML, Ping G, Plathow C, et al. Small molecule receptor tyrosine kinase inhibitor of platelet-derived growth factor signaling (SU9518) modifies radiation response in fibroblasts and endothelial cells. *BMC Cancer*. 2006;6. doi:10.1186/1471-2407-6-79
32. Sakurai E, Ozeki H, Kunou N, Ogura YJOR. Effect of particle size of polymeric nanospheres on intravitreal kinetics. *Ophthalmic Res*. 2001;33(1):31–36. doi:10.1159/000055638
33. Zhao J, Zhang X, Sun X, et al. Dual-functional lipid polymeric hybrid pH-responsive nanoparticles decorated with cell penetrating peptide and folate for therapy against rheumatoid arthritis. *Eur J Pharm Biopharm*. 2018;130:39–47. doi:10.1016/j.ejpb.2018.06.020
34. Zakarija A, Soff G. Update on angiogenesis inhibitors. *Curr Opin Oncol*. 2005;17(6):578–583. doi:10.1097/01.cco.0000183672.15133.ab
35. Wu Y, Zhong Z, Huber J, et al. Anti-vascular endothelial growth factor receptor-1 antagonist antibody as a therapeutic agent for cancer. *Clin Cancer Res*. 2006;12(21):6573–6584. doi:10.1158/1078-0432.CCR-06-0831
36. Voravud N, Charuruk N. Tumor angiogenesis. *J Med Associat Thai*. 1999;82(4):394.